Accepted for publication in AJ
Preprint typeset using LaTeX style emulateapj v. 11/12/01

THE 2MASS WIDE-FIELD T DWARF SEARCH. II. DISCOVERY OF THREE T DWARFS IN THE SOUTHERN HEMISPHERE

Adam J. Burgasser[1,2], Michael W. McElwain[1], & J. Davy Kirkpatrick[3]
Accepted for publication in AJ

ABSTRACT

We present the discovery of three new Southern Hemisphere T dwarfs identified in the Two Micron All Sky Survey. These objects, 2MASS 0348−6022, 2MASS 0516−0445, and 2MASS 2228−4310, have classifications T7, T5.5, and T6.5, respectively. Using linear absolute magnitude/spectral type relations derived from T dwarfs with measured parallaxes, we estimate spectrophotometric distances for these discoveries; the closest, 2MASS 0348−6022, is likely within 10 pc of the Sun. Proper motions and estimated tangential velocities are consistent with membership in the Galactic disk population. We also list Southern Hemisphere T dwarf candidates that were either not found in subsequent near-infrared imaging observations and are most likely uncatalogued minor planets, or have near-infrared spectra consistent with background stars.

Subject headings: Galaxy: solar neighborhood — infrared: stars — stars: individual (2MASS J03480772−6022270, 2MASS J05160945−0445499, 2MASS J22282889−4310262) — stars: low mass, brown dwarfs

1. INTRODUCTION

T dwarfs are substellar objects whose near-infrared spectra exhibit characteristic signatures of H_2O and CH_4 (Burgasser et al. 2002; Geballe et al. 2002). They comprise the coolest class of brown dwarfs currently known, with effective temperatures $T_{eff} \lesssim 1300$–1500 K (Burgasser et al. 2002; Dahn et al. 2002, and references therein). Their atmospheric properties are therefore quite similar to class III and IV extra-solar giant planets (EGPS; Sudarsky, Burrows, & Pinto 2000), but are more easily studied without the obscuration of a bright host star. Indeed, EGP atmospheric models have advanced in parallel with isolated brown dwarf models, as the latter differ only in the absence of an external radiating source (Seager & Sasselov 1998, 2000; Sudarsky, Burrows, & Pinto 2000; Baraffe et al. 2003). The observed properties of T dwarfs have served to constrain these models. The currently known collection of nearby T dwarfs are also useful for studies of the substellar population in the Solar Neighborhood and the substellar initial mass function (Burgasser 2001). Finally, as these objects do not significantly process their initial Hydrogen supply to heavier metals[4], they may be used as a tracer population of the chemical history of the Galaxy, as long as temperature, gravity, and metallicity diagnostics can be disentangled.

We have initiated a wide-field search for T dwarfs in the Two Micron All Sky Survey (Skrutskie et al. 1997, hereafter 2MASS), as described in Burgasser et al. (2003b, hereafter Paper I). 2MASS, which covers the entire sky, is an ideal survey for finding T dwarfs in the Solar Neighborhood, as the spectral energy distributions of these objects peak in the J, H, and K_s photometric bands sampled by the survey. The optical/near-infrared colors of T dwarfs are also extremely red ($R-J \gtrsim 9$; Golimowski et al. 1998); hence, photographic plate surveys, which also cover the whole sky, cannot detect T dwarfs much farther than a few parsecs from the Sun (Scholz et al. 2003). 2MASS is particularly useful for finding T dwarfs in the Southern Hemisphere, as it is more sensitive than the Deep Near-Infrared Survey of the Southern Sky (Epchtein et al. 1997), and there is as yet no equivalent to the Sloan Digital Sky Survey (York et al. 2000, hereafter SDSS) at southern latitudes.

In this article, we present the discovery of three new T dwarfs in the Southern Hemisphere, 2MASS 0348−6022, 2MASS 0516−0445, and 2MASS 2228−4310[5]. In § 2 we review the identification of these T dwarfs through confirmation imaging and spectroscopic observations obtained using the Ohio State InfraRed Imager/Spectrometer (Depoy et al. 1993, hereafter OSIRIS), mounted on the CTIO 4m Blanco Telescope. In § 3, we analyze the spectra of these and three other previously identified T dwarfs, 2MASS 0243−2453, 2MASS 0415−0935, and SDSS 0423−0414 (Burgasser et al. 2002; Geballe et al. 2002), also observed with OSIRIS. Including the latter sources into a suite of spectral standards, we classify the new T dwarfs and estimate their spectrophotometric distances. We also examine the kinematics of the three discoveries. Results are summarized in § 4.

2. OBSERVATIONS OF T DWARF CANDIDATES

2.1. *Imaging Observations*

[1] Department of Astronomy & Astrophysics, University of California at Los Angeles, Los Angeles, CA, 90095-1562; adam@astro.ucla.edu, mcelwain@astro.ucla.edu

[2] Hubble Fellow

[3] Infrared Processing and Analysis Center, M/S 100-22, California Institute of Technology, Pasadena, CA 91125; davy@ipac.caltech.edu

[4] Exhaustive Deuterium and Lithium burning occur in Solar metallicity brown dwarfs more massive than 0.013 and 0.065 $M_\odot$, respectively (Burrows et al. 2001).

[5] Throughout the text, we adopt shorthand notation for 2MASS and SDSS sources, 2MASS/SDSS hhmm±ddmm. Full designations are listed in Tables 1–3.

Selection of T dwarf candidates from the 2MASS Working Point Source Database (WPSD) are discussed in detail in Paper I. Our color constraints – $J - H \leq 0.3$ or $H - K_s \leq 0$, and no optical counterpart in the USNO A2.0 catalogue (Monet et al. 1998) or visible on Digitized Sky Survey (DSS) plates – result in some contamination by asteroids, as discussed in Burgasser et al. (2002). We specifically exclude objects associated with known minor planets in the 2MASS catalog, but uncatalogued ones are likely to be present. To eliminate these sources, we imaged a subset of our candidate pool with OSIRIS in the J-band during 20–24 September 2002 (UT). Conditions during this period ranged from clear and dry (20 and 24 September) to light cirrus and clouds (21–23 September), and seeing was poor ($\gtrsim 1\farcs5$) on 20 and 23 September but excellent ($\lesssim 1''$) on the remaining nights. Pairs of 15 sec integrations were obtained for each object, dithered 10–20″ between exposures. The sensitivity of these images was verified to be greater than that of the 2MASS survey, which has a J-band S/N = 10 completeness limit of 15.8 (Cutri et al. 2003), implying that any stationary sources should have been recovered.

As in Burgasser et al. (2002), a number of sources were not seen in the OSIRIS images; these are listed in Table 1, with updated designations and photometry from the 2MASS All Sky Data Release (Cutri et al. 2003, hereafter, 2MASS ADR). A few sources were identified as unflagged image artifacts arising from electronic feedback in the quadrant readout of the 2MASS NICMOS3 detectors ("star echo"; see sect. IV.7 in Cutri et al. 2003). Eleven sources were subsequently identified as known minor planets by searching a 30″×30″ region around the positions of each unconfirmed source at the corresponding epoch of observation in the Small Body catalog maintained by the Jet Propulsion Laboratory Solar System Dynamics Group[6]. We note that about half of these 2MASS asteroid detections precede their discovery. It is logical, therefore, that most of the remaining unconfirmed sources are uncatalogued minor planets, given that their near-infrared colors closely match those of known asteroids (Sykes et al. 2002) and that they are generally found at low ecliptic latitudes. Curiously, a handful of these probable minor planets are found at relatively high ecliptic latitudes, $25° \lesssim |\beta| \lesssim 40°$. We cannot rule out the possibility of any of these sources being eruptive or otherwise variable events.

2.2. *Spectroscopic Observations*

For sources that reappeared in the OSIRIS images, we obtained spectra during the same run using the OSIRIS cross-dispersed gratings. Use of the single diffraction grating blazed at 6.6 μm with the 120 lines mm^{-1} grating and f/2.8 camera provides simultaneous, moderate resolution ($\lambda/\Delta\lambda \sim 1200$) spectroscopy from 1.2–2.35 μm in four orders: J (5^{rd} and 6^{th}), H (4^{th}), and K (3^{th}). Resolution on the 0.″403 pixel^{-1} chip ranges from 4.4 to 8.8 Å pixel^{-1}.

Table 2 summarizes the observations, which also included three known T dwarfs: 2MASS 0243−2453, 2MASS 0415−0935, and SDSS 0423−0414 (Burgasser et al. 2002; Geballe et al. 2002). Targets were acquired in imaging mode and placed into a $1\farcs2 \times 30''$ slit. Observations were made in sets of 5 exposures dithered 4–5″ along the slit, with individual integrations of 300 sec per exposure. B and A dwarf stars, chosen for their lack of metal lines at moderate resolution, were observed near the target objects for flux calibration and telluric corrections. Spectral lamps reflected off of the 4m dome spot were observed each night for pixel response calibration, and a series of dark frames with identical exposure times as the spectral flats were also obtained to remove detector bias.

Data reduction consisted of initially trimming the science images to eliminate vignetted regions; dividing by a normalized, dark-subtracted flat field (constructed from a median combination of the spectral lamp and bias exposures); and correcting for bad pixels by interpolation, using a mask created from flat-field and bias frames. Images were then pairwise subtracted to eliminate sky background and dark current. Curvature of the dispersion lines was determined by tracing the spectra of the standard stars, and this trace was used as a template for the target spectra. Both standard and object spectra were extracted by summing 8–12 columns (depending on seeing conditions) along each row after subtracting off the median background in that row. Individual spectra from each order were then scaled by a multiplicative factor and combined by averaging, rejecting 3σ outliers in each spectral bin. Wavelength calibration was done with the telluric OH lines, using identifications from Olivia & Origlia (1992). A telluric correction was computed for each target/standard pair by interpolating over H_2O absorption features in the standard star spectra and ratioing these spectra with the uncorrected standard spectra. A smoothed flux correction was then calculated by interpolating over Hydrogen Paschen and Brackett lines in the telluric-corrected standard spectra and multiplying by the appropriate blackbody (Tokunaga 2000). Finally, the flux-calibrated spectral orders were combined by first scaling each order to match overlap regions (typically 1.28–1.30, 1.53–1.55, and 1.95–1.97 μm), and then correcting the combined spectra to 2MASS H-band magnitudes. Note that the overlap between the H- and K-band orders falls within the 1.9 μm H_2O band; because of this, we generally applied the same scaling corrections to both orders.

The majority of sources observed appear to be late-type (KM) background stars based on the presence of weak H_2O absorption and relatively featureless H-band spectra. This is consistent with their positions on the near-infrared color-color diagram in Figure 1 (which plots revised photometry from the 2MASS ADR[7]), within the substantial color uncertainties; c.f., the M dwarf and giant tracks of Bessell & Brett (1988). Furthermore, their faint magnitudes ($15.5 \lesssim J \lesssim 16$) imply optical/near-infrared color limits ($R - J > 4$–5, based on no detection in DSS photographic plates; Reid et al. 1991) consistent with late-type stars. In some cases these identifications were confirmed spectroscopically by comparison to near-infrared data of known M dwarfs obtained in prior OSIRIS campaigns

[6] Asteroid identifications were made using the Small-Body Search Tool, http://ssd.jpl.nasa.gov/cgi-bin/sb_search.

[7] The ADR colors for many of our candidates are outside of our original search constraints, which are based on 2MASS WPSD data. These differences are due to the improved photometric calibration of 2MASS J-band data in the ADR, which compensates for short (hourly) variations in telluric opacity that influence the broad J-band filter employed in this survey. See Cutri et al. (2003) for further details.

(Burgasser et al. 2002). None of the brighter background objects appear to be L dwarfs based on similar comparisons. Adequate spectral comparison for many of the spectra was not possible, however, due to low signal-to-noise ratio data ($\sim$ 5-10 at J-band in the worst cases), although it is clear that these faint objects are not T dwarfs. We forego detailed classification of background sources as it is beyond the scope of this paper, and identify them simply as late-type stars. We do, however, identify one candidate, 2MASS 2005−1056, as LHS 483, a DC9 white dwarf (McCook & Sion 1999, and references therein) with substantial proper motion ($\mu = 1\farcs08$ yr^{-1}; Luyten 1979). This object was not initially recognized as a background proper motion star because of the small epoch difference between the available DSS plates (2.1 yrs[8]). A second source, 2MASS 0533−0633, appears to be a reddened, mid- to late-type M dwarf based on its somewhat stronger H_2O bands, weak 1.23 μm FeH absorption, 1.25 μm K I doublet lines, and red near-infrared spectral slope. This source is also aligned with a small molecular clump just south of the Orion Nebular Cloud (Bally et al. 1987; Carpenter 2001, ONC). Its late-type dwarf spectrum and proximity to the 1–2 Myr ONC star-forming region (Hillenbrand 1997) suggests that it could be a young brown dwarf.

3. NEW T DWARFS

3.1. *Spectral Analysis*

We spectroscopically confirm three objects as T dwarfs: 2MASS 0348−6022, 2MASS 0516−0445, and 2MASS 2228−4310. Astrometric and photometric properties are listed in Table 3, and 2MASS and DSS images of each source ($5'\times5'$ field) are shown in Figure 2. Calibrated spectral data are shown in Figure 3, along with data for 2MASS 0243−2453, 2MASS 0415−0935, and SDSS 0423−0414. Note that data for 2MASS 0348−6022 and 2MASS 0516−0445 have been combined from multiple nights to improve signal-to-noise. All six T dwarfs show distinct CH_4 bands at 1.1, 1.3 (blue and red slopes of the 1.27 μm J-band peak), 1.6, and 2.2 μm; H_2O bands at 1.3 and 1.7 μm; and K I absorption lines at 1.2432 and 1.2522 μm. The spectrum of SDSS 0423−0414 shows some indication of CO absorption at 2.3 μm. The strength of the CH_4 and H_2O bands in the three new discoveries are consistent with late-type T dwarfs (Burgasser et al. 2002; Geballe et al. 2002).

Figure 4 displays the 1.19 to 1.33 μm region of the spectra in Figure 3, highlighting the 1.2432/1.2522 μm K I doublet lines. These lines are prominent in early- and mid-type T dwarf spectra (as well as late-type M and L dwarfs), peaking in strength around spectral type T5–T5.5, then fading in the later dwarfs (Burgasser et al. 2002). We measured pseudo-equivalent widths[9] (pEWs) for these lines by integrating over the line profiles; see Burgasser et al. (2002). Results are listed in Table 4. Values decrease monotonically from roughly 12 to 4 Å for the 1.2432 μm line and 16 to 6.5 Å for the 1.2522 μm line over spectral types T5.5 to T7, consistent with previously observed trends. Upper pEW limits of roughly 2 Å are found for the K I lines of the latest-type T dwarf 2MASS 0415−0935.

3.2. *Classification*

We derived spectral types for the three discoveries using the classification scheme of Burgasser et al. (2002). The top of Table 5 lists spectral ratio values of observed T dwarf standards, including new measurements for SDSS 0423−0414, 2MASS 0243−2453, and 2MASS 0415−0935 (our T0, T6, and T8 standards, respectively), and measurements using OSIRIS data for SDSS 1254−0122 (Leggett et al. 2000, T2), 2MASS 0559−0414 (Burgasser et al. 2000b, T5), and 2MASS 0727+1710 (Burgasser et al. 2002, T7) from Burgasser et al. (2002). We make use of the H_2O-B, CH_4-A, and CH_4-B indices only, due to the wavelength limits of the spectral data (obviating the the H_2O-A index), poor signal-to-noise at K-band (obviating the CH_4-C, and 2.11/2.07 indices) and possible uncertainties in the individual band calibration (obviating the H/J and K/J color indices). As can be seen in Table 5, the three remaining indices are monotonic with spectral type for the standards.

Spectral ratios of our discoveries are listed at the bottom of Table 5. For each ratio, we assigned a whole or half subtype based on the closest match to the standard values. Final subtypes were derived from the average of these individual ratio types, which for each object differ by less than ±1 subclass. Furthermore, individual spectra for 2MASS 0348−6022 and 2MASS 0516−0445 obtained on separate nights yield identical types within ±0.5 subclasses. Therefore, we assert that our classifications are accurate to within 0.5 subclasses despite the limited suite of spectral ratios employed. Derived spectral types are T7 for 2MASS 0348−6022, T5.5 for 2MASS 0516−0445, and T6.5 for 2MASS 2228−4310. These mid- to late-type classifications are consistent with their relatively blue near-infrared colors.

3.3. *Distance Estimates*

Distance estimates for our new discoveries can be made using their spectral types, 2MASS photometry, and the absolute magnitudes of T dwarfs with measured parallaxes. We first compared 2MASS M_J, M_H, and M_{K_s} versus spectral type (SpT) for T dwarfs typed T5 and later using parallax data from Dahn et al. (2002); Tinney, Burgasser, & Kirkpatrick (2003); and F. Vrba (2002, private communication). Excluding the known binaries 2MASS 1225−2739AB and 2MASS 1534−2952AB (Burgasser et al. 2003c) and Gliese 229B (Nakajima et al. 1995; not detected by 2MASS), we derive the following linear relations over the range T5 to T8:

$$\begin{aligned} M_J &= (10.00\pm0.12) + (0.84\pm0.02)\times\mathrm{SpT} \\ M_H &= (9.60\pm0.18) + (0.88\pm0.03)\times\mathrm{SpT} \\ M_{K_s} &= (8.7\pm0.3) + (0.98\pm0.05)\times\mathrm{SpT}, \end{aligned} \quad (1)$$

where SpT(T5) = 5, SpT(T8) = 8, etc. Based on these relations, we derived distance estimates for each source in

[8] We note that Bakos, Sahu, & Németh (2002) derive $\mu = 6\farcs82$ yr^{-1} for LHS 483 but cite the value as highly uncertain because of the small DSS epoch difference. From our imaging observations and 2MASS data (see §3.4) we derive $\mu = 0\farcs98\pm0\farcs03$ yr^{-1}, roughly consistent with Luyten's measurement.

[9] The presence of overlying opacity throughout the near-infrared prevents the measurement of "true continuum" for computing equivalent widths; hence, the reported measurements are relative to the local, or "pseudo"-continuum.

each band assuming spectral type uncertainties of ±0.5 subclasses. The mean distances and standard deviations are 9±4, 34±13, and 12±4 pc for 2MASS 0348−6022, 2MASS 0516−0445, and 2MASS 2228−4310, respectively. It is not surprising that the first object, which has the latest classification and brightest apparent magnitudes, is likely to be less than 10 pc from the Sun, unless it is an unresolved multiple system. However, parallax observations are required to verify these rather uncertain estimates.

3.4. *Proper Motions*

Proper motions for the T dwarf discoveries were measured between the 2MASS and follow-up OSIRIS images following the technique of Burgasser et al. (2003a). First, astrometric calibrations of each OSIRIS field, of the form

$$\begin{aligned} \alpha &= \alpha_o + Ax + By \\ \delta &= \delta_o + Cx + Dy, \end{aligned} \quad (2)$$

(x and y are pixel coordinates on the OSIRIS images) were made by linear regression using the 2MASS coordinates of 6–8 background sources within 2.′5 of each T dwarf. Background sources were verified to show consistent positions between the two epochs (which span 3.1–4.1 yr) to within three times the astrometric fit uncertainties, roughly 0.″05–0.″1. Positions for the T dwarfs on the OSIRIS images were then calculated and compared to the original 2MASS coordinates.

Results are listed in Table 3. As expected from their relative proximity, all of these sources have statistically significant proper motions. Their tangential velocities (V_t) are relatively modest, however, ranging from 17 to 55 km s^{-1}. These values are similar to the median for disk dwarfs (39 km s^{-1}; Reid & Hawley 2000) and comparable to or less than the median for field late-type M and L dwarfs (22 km s^{-1}; Gizis et al. 2000). Hence, the kinematics of these three T dwarfs are consistent with, but not restricted to, membership in the Galactic disk.

4. SUMMARY

We have identified three new southern T dwarfs using the 2MASS survey. These objects are important additions to the sample of nearby stars and brown dwarfs; indeed, one object, if it is single, is likely to be closer than 10 pc from the Sun. Spectroscopic observations yield classifications ranging from T5.5 to T7, and measured K I pEWs support the observed trend of decreasing line strength with spectral type for mid- to late-type T dwarfs. All three objects have small to moderate proper motions and tangential velocities, consistent with membership in the Galactic disk. With roughly 70% of the Southern Hemisphere portion of our 2MASS T Dwarf search sample now completed and 13 T dwarfs so far identified (Burgasser et al. 1999, 2000a,b, 2002), we expect to uncover another 5–6 mid- to late-type T dwarfs over the remaining portion of this part of the sky to $J = 16$.

We thank our Telescope Operator Sergio Pizarro and Support Scientist Nicole van der Bliek for their assistance at the telescope, and Kelle Cruz for her presence during the observations. We also thank our anonymous referee for her/his rapid and thorough examination of our submitted manuscript. A. J. B. acknowledges support by NASA through Hubble Fellowship grant HST-HF-01137.01 awarded by the Space Telescope Science Institute, which is operated by the Association of Universities for Research in Astronomy, Inc., for NASA, under contract NAS 5-26555. This research has made use of the SIMBAD database, operated at CDS, Strasbourg, France. AAO and SERC images were obtained from the Digitized Sky Survey image server maintained by the Canadian Astronomy Data Centre, which is operated by the Herzberg Institute of Astrophysics, National Research Council of Canada. This publication makes use of data from the Two Micron All Sky Survey, which is a joint project of the University of Massachusetts and the Infrared Processing and Analysis Center, funded by the National Aeronautics and Space Administration and the National Science Foundation. 2MASS data were obtained through the NASA/IPAC Infrared Science Archive, which is operated by the Jet Propulsion Laboratory, California Institute of Technology, under contract with the National Aeronautics and Space Administration.

REFERENCES

Bakos, G. Á., Sahu, K. C., & Németh, P. 2002, ApJS, 141, 187
Bally, J., Stark, A. A., Wilson, R. W., & Langer, W. D. 1987, ApJ, 312, L45
Baraffe, I., Chabrier, G., Barman, T., Allard, F., & Hauschildt, P. H. 2003, A&A, in press (astro-ph/0302293)
Bessell, M. S., & Brett, J. M. 1988, PASP, 100, 1134
Burgasser, A. J. 2001, Ph.D. Thesis, California Institute of Technology
Burgasser, A. J., Kirkpatrick, J. D., Burrows, A., Liebert, J., Reid, I. N., Gizis, J. E., McGovern, M. R., Prato, L., & McLean, I. S. 2003a, ApJ, 592, in press (astro-ph/0304174)
Burgasser, A. J., Kirkpatrick, J. D., McElwain, M. W., Cutri, R. M., Burgasser, A. J., & Skrutskie, M. F. 2003b, AJ, 125, 850 (Paper I)
Burgasser, A. J., Kirkpatrick, J. D., Reid, I. N., Brown, M. E., Miskey, C. L., & Gizis, J. E. 2003c, ApJ, 586, 512
Burgasser, A. J., et al. 1999, ApJ, 522, L65
—. 2000a, ApJ, 531, L57
—. 2000b, AJ, 120, 1100
—. 2002, ApJ, 564, 421
Burrows, A., Hubbard, W. B., Lunine, J. I., & Liebert, J. 2001, Rev. of Modern Physics, 73, 719
Burrows, A., et al. 1997, ApJ, 491, 856
Carpenter, J. M. 2001, AJ, 120, 3139
Cutri, R. M., et al. 2003, Explanatory Supplement to the 2MASS All Sky Data Release, http://www.ipac.caltech.edu/2mass/releases/allsky/doc/explsup.html
Dahn, C. C., et al. 2002, AJ, 124, 1170
Depoy, D. L., Atwood, B., Byard, P. L., Frogel, J., & O'Brien, T. P. 1993, in Proceedings of SPIE, Vol. 1946, ed. A. M. Fowler (Bellingham: SPIE), 667
Epchtein, N., et al. 1997, The Messenger, 87, 27
Geballe, T. R., et al. 2002, ApJ, 564, 466
Gizis, J. E., Monet, D. G., Reid, I. N., Kirkpatrick, J. D., Liebert, J., & Williams, R. 2000, AJ, 120, 1085
Golimowski, D. A., Burrows, C. S., Kulkarni, S. R., Oppenheimer, B. R., & Brukardt, R. A. 1998, AJ, 115, 2579
Hillenbrand, L. A. 1997, AJ, 113, 1733
Kirkpatrick, J. D., Reid, I. N., Liebert, J., Gizis, J. E., Burgasser, A. J., Monet, D. G., Dahn, C. C., Nelson, B., & Williams, R. J. 2000, AJ, 120, 447
Leggett, S. K., Allard, F., Geballe, T., Hauschildt, P. H., & Schweitzer, A. 2001, ApJ, 548, 908
Leggett, S. K., et al. 2000, ApJ, 536, L35
Luyten, W. J. 1979, LHS Catalogue: A Catalogue of Stars with Proper Motions Exceeding 0.″5 Annually (Minneapolis: Univ. Minn. Press)
McCook, G. P., & Sion, E. M. 1999, ApJS, 121, 1
Monet, D. G., et al. 1998, USNO-A2.0 Catalog (Flagstaff: USNO)

Nakajima, T., Oppenheimer, B. R., Kulkarni, S. R., Golimowski, D. A., Matthews, K., & Durrance, S. T. 1995, Nature, 378, 463
Olivia, E., & Origlia, L. 1992, A&A, 254, 466
Pavlenko, Ya., Zapatero Osorio, M. R., & Rebolo, R. 2000, A&A, 355, 245
Reid, I. N., & Hawley, S. L. 2000, New Light on Dark Stars (Chichester: Praxis)
Reid, I. N., et al. 1991, PASP, 103, 661
Sanchez-Lavega, A. 2001, A&A, 377, 354
Scholz, R.-D., McCaughrean, M. J., Lodieu, N., & Kuhlbrodt, B. 2003, A&A, 398, L29
Seager, S., & Sasselov, D. D. 1998, ApJ, 502, L157
—. 2000, ApJ, 537, 916
Skrutskie, M. F., et al. 1997, in The Impact of Large-Scale Near-IR Sky Surveys, ed. F. Garzon (Dordrecht: Kluwer), p. 25
Stephens, D. C., Marley, M. S., Noll, K. S., & Chanover, N. 2001, ApJ, 556, L97
Strom, K. M., Strom, S. E., & Merrill, K. M. 1993, ApJ, 412, 233
Sudarsky, D., Burrows, A., & Pinto, P. 2000, ApJ, 538, 885
Sykes, M. V., Cutri, R. M., Fowler, J. W., Nelson, B., Tholen, D. J., Skrutskie, M. F., & Price, S. 2002, in Proceedings of the ACM 2002 Conference, ed. B. Warmbein, ESA-SP-500, p. 481
Tinney, C. G., Burgasser, A. J., & Kirkpatrick, J. D. 2003, AJ, in press (astro-ph/0304339)
Tokunaga, A. T. 2000, in Allen's Astrophysical Quantities, Fourth Edition, ed. A. N. Cox (New York: Springer-Verlag), p. 151
York, D. G., et al. 2000, AJ, 120, 1579

TABLE 1
T DWARF CANDIDATES ABSENT IN FOLLOW-UP OSIRIS IMAGES.

Object[a] (1)	β (°) (2)	2MASS Observations[b] UT Date (3)	J (4)	$J-H$ (5)	$H-K_s$ (6)	Identification[c] (7)
2MASS J01315876−1259435	−21	2000 Oct 23	15.86±0.07	0.14±0.16	0.15±0.24	
2MASS J01392545−0258486	−12	1998 Sep 23	15.68±0.06	0.46±0.12	−0.20±0.20	2001 KY8
2MASS J01432550−1240101	−22	2000 Oct 10	15.79±0.07	0.40±0.11	−0.14±0.21	
2MASS J01492365−1945149	−29	1998 Aug 10	15.53±0.05	0.29±0.09	0.15±0.14	
2MASS J01542969−1258435	−23	1998 Aug 20	15.50±0.05	0.53±0.08	−0.13±0.16	2000 EY156
2MASS J02061785+0456321	−7	2000 Nov 27	15.96±0.08	0.06±0.21	0.21±0.28	2000 SX124
2MASS J02100930+0908316	−4	2000 Sep 28	15.76±0.06	0.37±0.11	−0.04±0.22	
2MASS J02253536−5539594	−63	1999 Oct 27	15.30±0.08	−0.20±0.16	< 0.86	Image artifact
2MASS J02525674−8020549	−72	2000 Oct 04	15.83±0.10	−0.03±0.21	< 0.94	Image artifact
2MASS J03014529−6055462	−70	1999 Nov 11	15.33±0.10	−0.44±0.21	< 1.37	Image artifact
2MASS J03184819−4216275	−57	1999 Sep 26	15.14±0.09	−0.90±0.24	< 0.86	Image artifact
2MASS J03295950−5446545	−69	1999 Nov 02	15.38±0.11	0.17±0.22	< 1.34	Image artifact
2MASS J03451647+1132394	−8	2000 Nov 25	15.77±0.07	0.57±0.11	−0.13±0.17	1990 QB3
2MASS J03594765+1341458	−7	1998 Nov 17	15.51±0.06	0.47±0.09	−0.15±0.16	
2MASS J19084533−3352087	−11	2000 Jul 20	15.86±0.06	0.26±0.13	0.31±0.19	
2MASS J19183027−3427382	−12	1998 Jul 25	15.63±0.05	0.03±0.14	0.39±0.20	
2MASS J19231778−4832099	−26	2000 Oct 12	15.71±0.09	−0.16±0.22	< 0.60	Image artifact
2MASS J19243027−4332438	−21	1999 Jul 14	15.96±0.09	0.26±0.18	0.35±0.22	1996 TP34
2MASS J19263511−3435565	−13	1998 Jul 26	15.89±0.09	0.05±0.21	0.38±0.29	
2MASS J19355972−2923351	−8	1998 Jul 05	15.91±0.09	0.22±0.17	−0.01±0.28	
2MASS J19492452−3201418	−11	2000 Aug 10	15.66±0.06	0.53±0.11	−0.03±0.17	2001 RZ
2MASS J19530053−3512193	−14	1999 Jul 15	15.52±0.06	0.47±0.09	−0.26±0.15	
2MASS J20153100−2958197	−10	1998 Aug 10	15.09±0.03	0.29±0.07	0.17±0.12	
2MASS J20180855−3250195	−13	1999 Sep 26	15.80±0.07	0.21±0.14	−0.15±0.28	
2MASS J20203953−3414209	−14	1999 Jun 13	15.89±0.09	0.22±0.16	0.14±0.25	
2MASS J20342244−3748127	−18	1998 Sep 08	15.83±0.06	0.40±0.11	−0.11±0.21	1989 TR2
2MASS J20352362−3858012	−20	1998 Sep 08	15.80±0.05	0.45±0.10	−0.22±0.21	
2MASS J20464656−2831162	−10	2000 Jul 24	15.38±0.05	0.29±0.09	0.03±0.14	
2MASS J20493283−4532443	−27	1999 Jul 26	15.97±0.07	0.19±0.15	0.37±0.22	
2MASS J20495554−3525083	−17	1999 Sep 09	15.96±0.09	0.27±0.15	0.24±0.21	
2MASS J20514464−3123264	−13	1999 Jul 09	15.93±0.06	0.38±0.11	−0.26±0.27	
2MASS J20533768−3227270	−14	1998 Aug 20	15.60±0.06	0.62±0.09	−0.14±0.14	1999 XN168
2MASS J20572107−3304186	−15	1998 Aug 20	16.00±0.07	0.56±0.14	−0.23±0.23	
2MASS J21035085−2237412	−6	2000 Aug 06	15.46±0.05	0.25±0.10	0.05±0.16	
2MASS J21050753−3122506	−14	1998 Aug 20	15.71±0.05	0.39±0.10	−0.02±0.18	
2MASS J21054515−3542535	−18	1998 Aug 20	15.67±0.04	0.58±0.08	−0.01±0.13	
2MASS J21090201−3725168	−20	1999 Aug 12	15.53±0.08	0.18±0.14	0.38±0.18	
2MASS J21113838−4133320	−24	1999 Sep 10	15.74±0.06	0.37±0.11	−0.06±0.19	
2MASS J21165349−3325598	−17	1998 Aug 15	15.80±0.06	0.43±0.14	−0.09±0.22	1999 WA1
2MASS J21170863−2441328	−8	1998 Aug 04	15.38±0.05	0.49±0.07	−0.02±0.12	2001 FP26
2MASS J21183794−2813093	−12	1998 Aug 04	15.85±0.06	0.57±0.11	−0.07±0.19	
2MASS J21285884−4249292	−26	1999 Aug 20	15.46±0.06	0.39±0.08	−0.02±0.14	
2MASS J21413332−2453233	−10	1998 Aug 12	15.73±0.06	0.39±0.09	−0.16±0.16	
2MASS J22050171−2658019	−14	2000 Jul 24	15.41±0.05	0.27±0.08	−0.19±0.16	
2MASS J22154587−2605584	−14	2000 Jul 24	15.53±0.05	0.29±0.09	0.04±0.15	
2MASS J22165310−2656329	−15	1998 Jul 31	15.43±0.06	0.05±0.13	0.09±0.20	
2MASS J22311396−3417156	−23	2000 Jul 24	14.53±0.03	0.29±0.05	0.00±0.07	
2MASS J22385056−5456370	−42	2000 Aug 02	15.98±0.09	0.13±0.19	0.21±0.27	
2MASS J22420219−3346098	−24	1999 Jul 26	15.56±0.05	0.43±0.09	−0.10±0.17	1997 YZ3
2MASS J22541137−4826135	−38	1999 Sep 21	15.97±0.08	0.14±0.13	0.35±0.23	

[a]All objects are listed with their 2MASS ADR Point Source Catalog source designations, given as "2MASS Jhhmmss[.]ss±ddmmss[.]s". The suffix conforms to IAU nomenclature convention and is the sexagesimal Right Ascension and declination at J2000 equinox.

[b]Photometry from the 2MASS ADR; note that some objects have revised photometry placing them outside of our original WPSD search constraints.

[c]Asteroid identifications are from the Small-Body Search Tool maintained by the Jet Propulsion Laboratory Solar System Dynamics Group: http://ssd.jpl.nasa.gov/cgi-bin/sb_search.

TABLE 2
LOG OF OSIRIS SPECTROSCOPIC OBSERVATIONS.

Object (1)	J[a] (2)	$J-K_s$[a] (3)	UT Date (4)	t (s) (5)	Airmass (6)	Calibrator (7)	SpT (8)	Identification (9)
2MASS J00231718−3346366	16.01±0.08	0.61±0.23	2002 Sep 23	1500	1.00	HD 6619	A1 V	Late-type star
2MASS J02053685−0853442	15.89±0.06	0.73±0.17	2002 Sep 20	1500	1.09	HD 13936	A0 V	Late-type star
2MASS J02431371−2453298	15.38±0.05	0.16±0.17	2002 Sep 24	1500	1.04	HD 20293	A5 V	T6 standard
2MASS J02485356−4951573	16.14±0.12	1.13±0.19	2002 Sep 22	1500	1.14	HD 17098	B9 V	Reddened star
2MASS J02512393−3842100	15.95±0.08	0.78±0.19	2002 Sep 22	1500	1.03	HD 17098	B9 V	Late-type star
2MASS J02560785−4311108	15.69±0.06	0.75±0.17	2002 Sep 24	1500	1.04	HD 20293	A5 V	Late-type star
2MASS J03164047−6202104	15.85±0.08	1.02±0.14	2002 Sep 22	1500	1.19	HD 22252	B8 V	Late-type star
2MASS J03480772−6022270	15.32±0.06	−0.28±0.24	2002 Sep 21	1500	1.19	HD 24863	A4 V	T dwarf
2MASS J04143647−6916594	15.72±0.07	0.89±0.16	2002 Sep 24	1500	1.31	HD 37935	B9.5 V	Late-type star
2MASS J04151954−0935066	15.70±0.06	0.27±0.21	2002 Sep 24	1500	1.08	HD 28763	A2/3 V	T8 standard
SDSSp J042348.57−041403.5	14.47±0.03	1.54±0.04	2002 Sep 23	1500	1.29	HD 30321	A2 V	T0 standard
2MASS J05160945−0445499	15.98±0.09	0.50±0.22	2002 Sep 21	1500	1.12	HD 33948	B5 V	T dwarf
			2002 Sep 22	1500	1.11	HD 37303	B1 V	
			2002 Sep 24	1500	1.11	HD 28763	A2/3 V	
2MASS J05335973−0633098	15.76±0.06	0.93±0.10	2002 Sep 22	1500	1.16	HD 37303	B8 V	Reddened M dwarf[b]
2MASS J17065753−0428539	15.96±0.09	0.53±0.20	2002 Sep 23	1500	1.38	HD 159170	A5 V	Late-type star
2MASS J18031154+1305281	16.03±0.09	0.85±0.18	2002 Sep 22	3000	1.52	HD 171975	B9 V	Late-type star
2MASS J19092267−8234478	15.52±0.06	0.74±0.13	2002 Sep 22	1500	1.67	HD 169904	B8 V	Late-type star
2MASS J19215777−6303224	15.62±0.05	0.66±0.14	2002 Sep 20	3000	1.21	HD 186837	B5 V	Late-type star
2MASS J19300878−4435012	15.96±0.08	1.06±0.14	2002 Sep 21	1500	1.03	HD 176425	A0 V	Late-type star
2MASS J19322282−6835592	16.00±0.09	0.97±0.16	2002 Sep 24	1500	1.28	HD 184586	A1 V	Late-type star
2MASS J19325619−4851162	15.99±0.09	1.01±0.15	2002 Sep 23	1500	1.25	HD 189388	A2/3 V	Late-type star
2MASS J19383909−2735379	15.97±0.08	0.62±0.21	2002 Sep 21	1500	1.02	HD 176425	A0 V	Late-type star
2MASS J19394892−5531025	15.87±0.08	0.51±0.18	2002 Sep 20	1500	1.19	HD 186837	B5 V	Late-type star
2MASS J19465571−3644491	15.58±0.07	0.72±0.14	2002 Sep 21	1500	1.07	HD 176425	A0 V	Late-type star[c]
2MASS J20014023−4111011	15.94±0.06	0.51±0.20	2002 Sep 20	1500	1.33	HD 189399	A2/3 V	Late-type star
2MASS J20053482−1056545	15.28±0.05	0.53±0.12	2002 Sep 22	1500	1.20	HD 202753	B5 V	LHS 483, white dwarf
2MASS J20364476+0335475	15.75±0.08	0.46±0.19	2002 Sep 23	1500	1.20	HD 198070	A0 Vn	Late-type star
2MASS J20425201−7924433	15.67±0.06	0.64±0.15	2002 Sep 21	1500	1.77	HD 203955	A0 V	Late-type star
2MASS J20592033+1752232	16.02±0.09	0.79±0.20	2002 Sep 24	1500	1.60	HD 207563	B2 V	Late-type star
2MASS J21264358−0926573	15.91±0.09	0.86±0.17	2002 Sep 22	1500	1.24	HD 215143	A0 Vn	Late-type star
2MASS J21301473−0720578	15.48±0.08	0.66±0.16	2002 Sep 20	1500	1.14	HD 186837	B5 V	Late-type star
2MASS J21393009−0928268	15.88±0.07	0.53±0.20	2002 Sep 22	1500	1.31	HD 215143	A0 Vn	Late-type star
2MASS J21443131+0327100	15.84±0.06	1.02±0.13	2002 Sep 23	1500	1.21	HD 198070	A0 Vn	Late-type star
2MASS J22282889−4310262	15.66±0.08	0.37±0.22	2002 Sep 24	3000	1.10	HD 220802	B9 V	T dwarf

[a]Photometry from the 2MASS ADR; note that some objects have revised photometry outside of our original WPSD search constraints.

[b]Candidate young brown dwarf in the Orion A complex (Strom, Strom, & Merrill 1993; Carpenter 2001).

[c]This object appeared much fainter at J-band when imaged with OSIRIS than as observed by 2MASS. It is possible that the 2MASS source is a chance alignment with an uncatalogued minor planet, or that this source is intrinsically variable.

TABLE 3
OBSERVED PROPERTIES OF THE NEW T DWARFS.

Object	Type	J	$J-H$	$H-K_s$	d_{sp}[a] (pc)	μ ($''$ yr^{-1})	θ ($^\circ$)	V_t (km s^{-1})
(1)	(2)	(3)	(4)	(5)	(6)	(7)	(8)	(9)
2MASS J03480772−6022270	T7	15.32±0.06	−0.24±0.16	−0.04±0.28	9±4	0.77±0.04	201±3	32±14
2MASS J05160945−0445499	T5.5	15.98±0.09	0.26±0.19	0.24±0.27	34±13	0.34±0.03	232±5	55±21
2MASS J22282889−4310262	T6.5	15.66±0.08	0.30±0.14	0.07±0.24	12±4	0.31±0.03	175±15	17±6

[a]Estimated spectrophotometric distance based on spectral type and 2MASS JHK_s photometry; see § 3.3.

TABLE 4
K I PSEUDO-EQUIVALENT WIDTHS.

		1.2432 μm		1.2522 μm	
Object	Type	λ_c (μm)	pEW (Å)	λ_c (μm)	pEW (Å)
(1)	(2)	(3)	(4)	(5)	(6)
SDSS 0423−0414	T0	1.243	6.4±0.8	1.252	6.6±1.0
2MASS 0516−0445[a]	T5.5	1.242	11.6±2.3	1.252	15.9±2.0
2MASS 0243−2453	T6	1.243	6.8±1.8	1.252	10.2±1.1
2MASS 2228−4310	T6.5	1.243	5.0±1.0	1.251	9.9±1.6
2MASS 0348−6022	T7	1.242	4.0±1.1	1.250	6.4±1.2
2MASS 0415−0935	T8	—	< 1.7	—	< 2.2

[a]Measured from combined spectrum.

TABLE 5
SPECTRAL RATIOS AND CLASSIFICATION ON THE BURGASSER ET AL. (2002) SCHEME.

Object	H_2O-B	CH_4-A	CH_4-B	SpT[a]
(1)	(2)	(3)	(4)	(5)
Standards				
SDSS 0423−0414	0.689	0.985	0.916	T0
SDSS 1254−0122[b]	0.559	0.943	0.826	T2
2MASS 0559−1404[b]	0.456	0.789	0.383	T5
2MASS 0243−2453	0.369	0.648	0.229	T6
2MASS 0727−1710[b]	0.332	0.509	0.133	T7
2MASS 0415−0935	0.267	0.429	0.062	T8
Discoveries				
2MASS 0348−6022	0.371(6)	0.541(7)	0.104(7/8)	T7
2MASS 0516−0445[c]	0.378(6)	0.812(5)	0.207(6)	T5.5
2MASS 2228−4310	0.285(7/8)	0.681(6)	0.228(6)	T6.5

[a]Adopted spectral type for standards; derived spectral type for discoveries, with uncertainty ±0.5 subclasses.

[b]Data from Burgasser et al. (2002).

[c]Measured from combined spectrum.

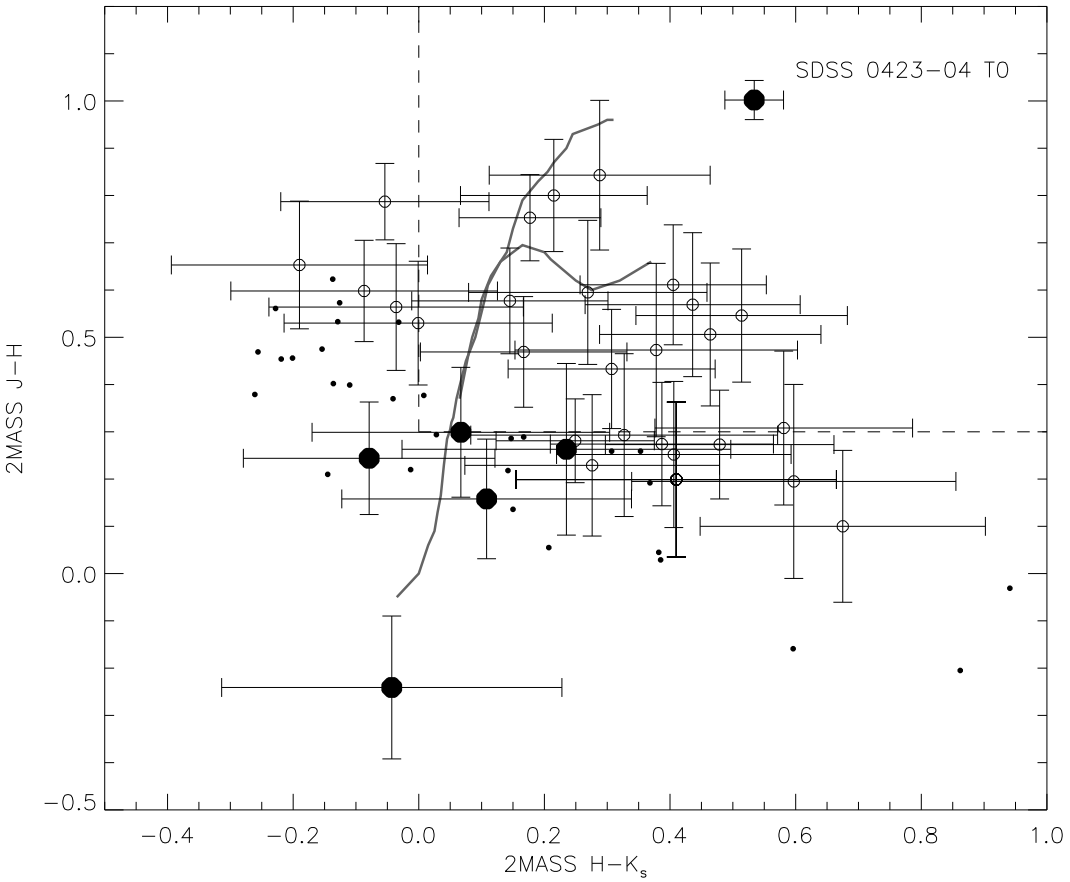

FIG. 1.— 2MASS near-infrared color-color diagram for observed T dwarfs and T dwarf candidates, with photometry from the 2MASS ADR. Small points indicate objects absent in follow-up OSIRIS images; open circles indicate background sources based on spectroscopic observations; large filled circles indicate the three new T dwarfs and the known T dwarfs 2MASS 0243−2453, 2MASS 0415−0935, and SDSS 0423−0414 (identified). Dwarf (lower) and giant (upper) tracks from Bessell & Brett (1988) are indicated by grey lines. Note that many of the background sources have revised 2MASS ADR colors outside of our original WPSD search constraints (dashed lines). The revised colors are consistent with their spectroscopic identifications as late-type background stars.

FIG. 2.— Findercharts for the T dwarf discoveries, showing AAO/SERC (R-band), and 2MASS (J- and K_s-bands) fields. Images are scaled to the same spatial resolution, $5'$ on a side, with North up and East to the left. A $10''$ box is centered on the position of the T dwarf in all images. *Note* : $Figure 2 is included as a separate jpeg file due to space considerations.$

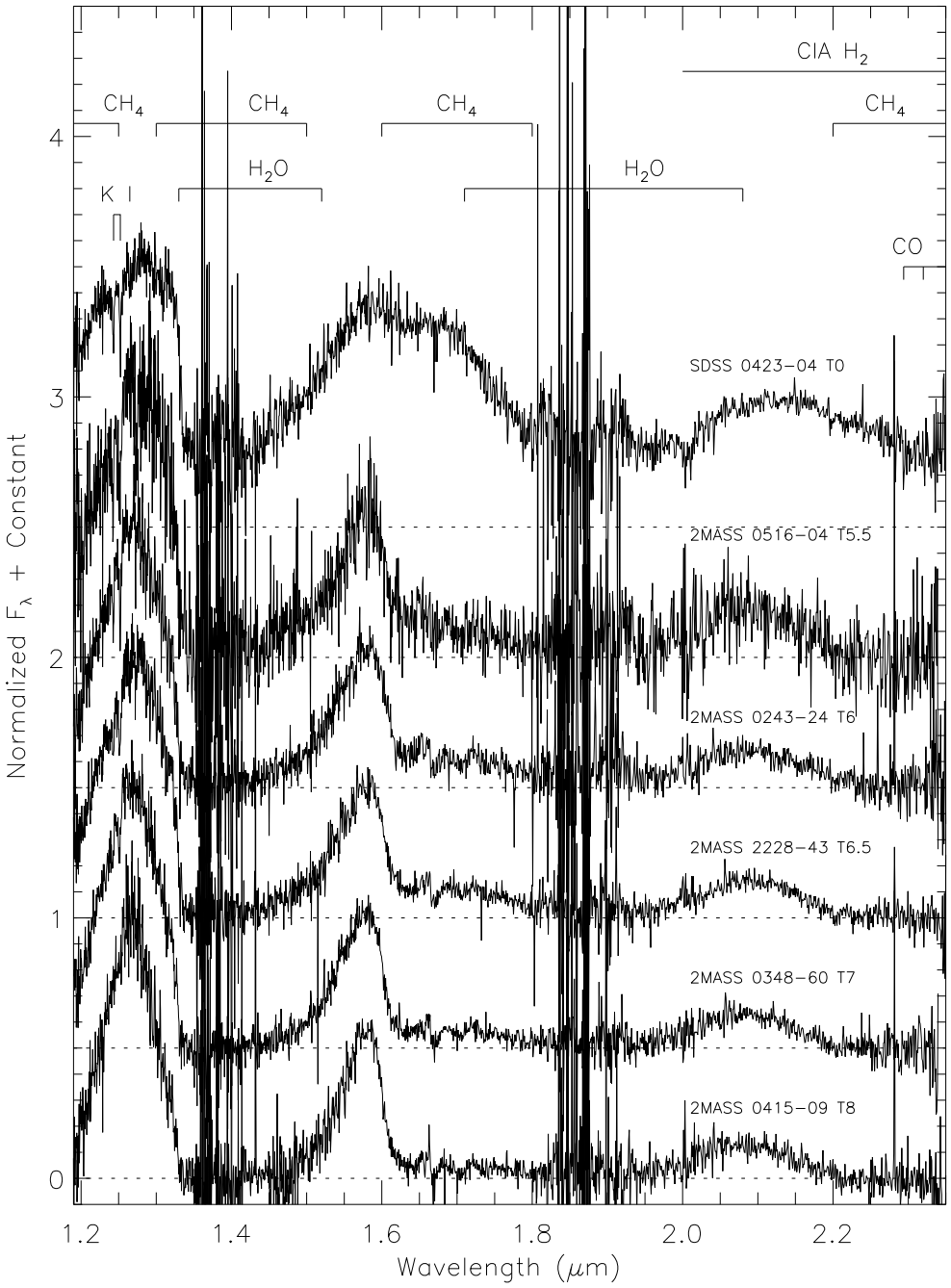

FIG. 3.— Reduced OSIRIS spectra of the observed T dwarfs in order of spectral type. Data are normalized at 1.2 μm and offset by a constant (dashed line). Major features of CH_4, H_2O, CO, and K I are identified, as well as the region most strongly affected by CIA H_2 absorption.

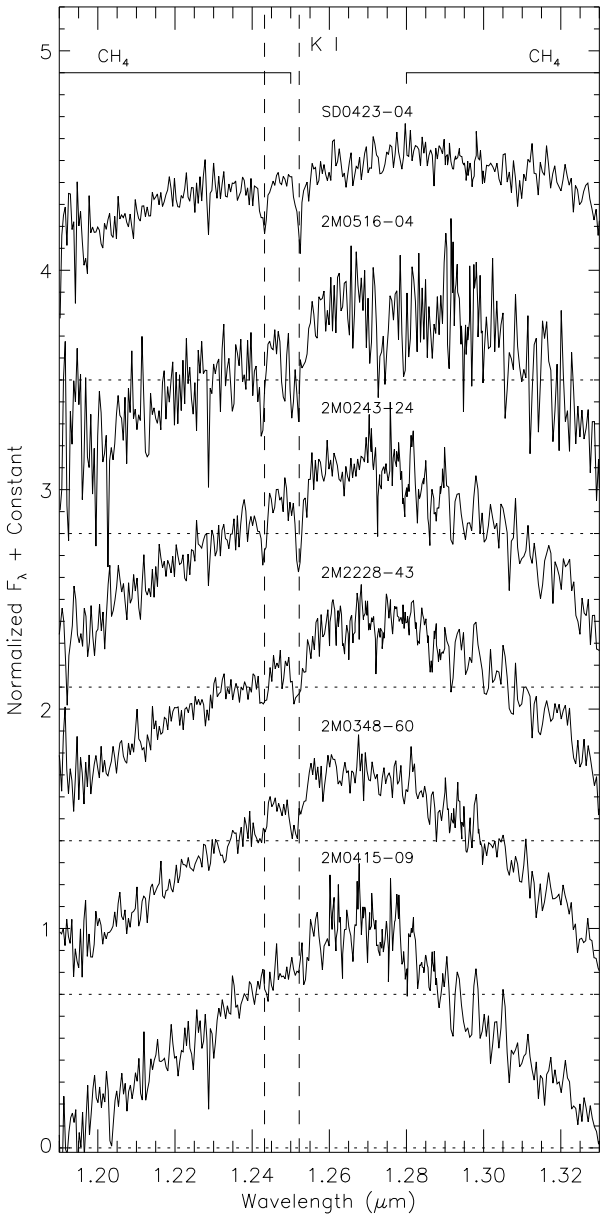

FIG. 4.— OSIRIS spectral data for the observed T dwarfs from 1.19 to 1.33 μm, highlighting the 1.2432/1.2522 μm K I doublet (vertical dashed lines). Spectra are scaled and offset as in Figure 3. Note that the feature at 1.27 μm in the spectra of 2MASS 0516−0445, 2MASS 0243−2453, and 2MASS 2228−4310 is an artifact of the data reduction.


This figure "Burgasser.fig2.jpg" is available in "jpg" format from:
http://arXiv.org/ps/astro-ph/0307374v1